



Macrocyclic triphenylamine based organic dyes for efficient dye-sensitized solar cells

Yun Zhao^a, Kejian Jiang^b, Wei Xu^a, Daoben Zhu^{a,*}

^a Beijing National Laboratory for Molecular Sciences, Organic Solids Laboratory, Institute of Chemistry, Chinese Academy of Sciences, Beijing 100190, PR China

^b Beijing National Laboratory for Molecular Sciences, Laboratory of New Materials, Institute of Chemistry, Chinese Academy of Sciences, Beijing 100190, PR China

ARTICLE INFO

Article history:

Received 7 June 2012

Received in revised form 4 August 2012

Accepted 10 August 2012

Available online 16 August 2012

Keywords:

Dye sensitized solar cells
Macrocyclic triphenylamine
Electron retardation
Organic dyes
Auxiliary electron donor

ABSTRACT

A novel class of organic D- π -A dyes employing macrocyclic triphenylamine dimer as electron donor was designed and synthesized for dye-sensitized solar cells. The prepared compounds showed high chemical and electrochemical stabilities as well as good long-wave absorption. Photovoltaic devices based on these dyes showed high open circuit voltage (higher than that of **N3**) and achieved a solar energy to electricity conversion efficiency of 6.31%. All the performances indicate the dyes containing macrocyclic triphenylamine dimer is a good candidate for dyes sensitized solar cells.

© 2012 Elsevier Ltd. All rights reserved.

1. Introduction

Dye-sensitized solar cells (DSSCs) have attracted intense interests for their high performance in converting solar energy to electricity at low cost. So far the best solar energy conversion efficiency of DSSCs based on Ru complexes exceed 10%.^{1,2} Recently, there are increasing interests in metal-free organic dyes due to their advantageous features, such as high molar extinction coefficients, easily modified molecular structure, and relatively low cost.³ The metal-free organic dyes commonly consist of donor, linker, and acceptor groups. Their various properties could be finely tuned by alternating independently or matching the different groups. Triphenylamine, fluorene, thiophene, indoline, merocyanine, coumarin, etc. have been employed as donor units in the development of metal-free sensitizers and exhibit promising device characteristics.^{3–6}

It has been found the incorporation of an auxiliary electron donor can bring about superior performance over the simple D- π -A configuration, in terms of bathochromically extended absorption spectra, enhanced molar extinction coefficients and more stabilized photoexcited states.^{7,4} Here, we would like to present two novel macrocycle derived organic dyes, each contained two triphenylamine units linked by vinylene bridges. In the macrocycle, the

triphenylamines are conjugated with each other, so the better intramolecular charge transfer, as well as strengthened electron donating ability can be expected.⁸ Thus, compared to the single bridge connected triphenylamine dimers, the macrocycle would have more advantages in stabilizing the initially formed radical cation by σ - π through-bond and through-space interactions,⁹ extending the absorption region, and preventing the direct charge recombination between TiO₂ and I₃⁻ by the bulky aryl group covering TiO₂ surfaces.^{10–12} The triphenylamine is chosen as donor unit due to its good electron donating ability, thermal, and chemical stabilities.¹³

2. Results and discussion

2.1. Molecular design

As shown in Fig. 1, we prepared the organic dyes **MC-T-CA** and **MC-HT-CA**, which contained thiophene linker with macrocyclic triphenylamine dimer as an electron donor and cyanoacrylic acid as an acceptor moiety. The synthetic procedure included well known reactions and gave a moderate yield. For **MC-T-CA**, the macrocycle moiety was coupled with 2-formylthiophene via Suzuki reaction, followed by conversion of the aldehyde group to cyanoacetic acid through Knoevenagel reaction in the presence of piperidine. The synthesis of **MC-HT-CA** was similar. However, during the Suzuki coupling reaction, the bulk center part of compound **6** made the reaction very difficult to be accomplished, and in the

* Corresponding author. Tel.: +86 10 6254 4083; fax: +86 10 6256 9349; e-mail addresses: zhaoyun@iccas.ac.cn (Y. Zhao), zhudb@iccas.ac.cn (D. Zhu).

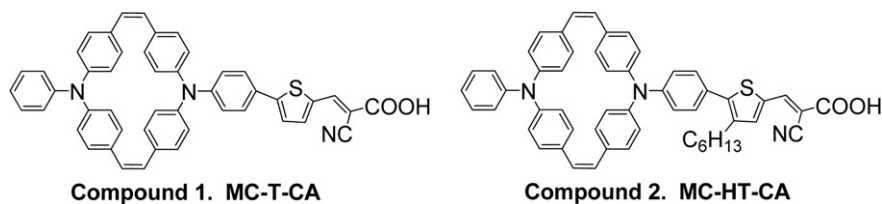
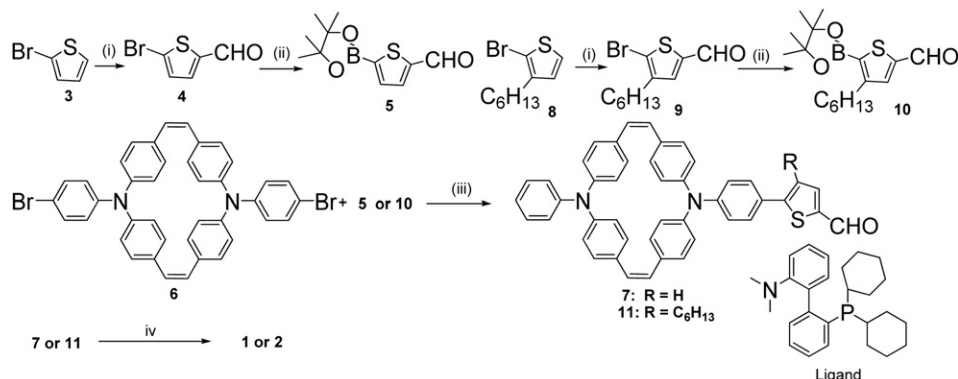


Fig. 1. Molecular structure of the organic dyes.

transmetalation procedure one of bromine atom was eliminated. Finally, we only got one-substituted product.¹⁴

2.2. General procedures

The synthetic procedure of compound **1** and **2** was shown in Scheme 1. All manipulations of air/moisture-sensitive materials were handled under nitrogen atmosphere using Schlenk techniques. Dioxane was distilled over sodium/benzophenone. Pyridine was distilled over NaOH. All reagents were used as received unless otherwise noted. ¹H NMR and ¹³C NMR spectra were obtained on Bruker Advance 400 or 600 spectrometers. EIMS measurements were performed on UK GCT-Micromass or SHIMADZU G-MS-QP2010 spectrometers. High-resolution mass spectrometry measurements (HRMS) were performed on UK GCT-Micromass spectrometers. Elemental analyses were carried out on a Carlo Erba 1106 elemental analyzer.



Scheme 1. Synthetic route to prepare the dyes **1** and **2**. Reagents and conditions: (i) DMF, POCl₃, 90 °C, 4 h, 84%; (ii) Pd(dppf)Cl₂, KOAc, bis(pinacolato)diboron, dioxane, 80 °C, 6 h; (iii) Pd(OAc)₂, Ligand, CsF, dioxane, 110 °C, 20 h, 23%; (iv) CNCH₂COOH, piperidine, CHCl₃, 70 °C, 6 h, 94%.

2.3. Electrochemical and photophysical data

Fig. 2 shows the absorption spectra of the triphenylamine macrocycle (MC) and the two dyes in CH₂Cl₂, and the cyclic voltammogram measurements are shown in Fig. 3. All the related photophysical data are summarized in Table 1. The LUMO levels of the two dyes were -3.02 and -3.00 eV, respectively, sufficiently higher in energy than the conduction band edge of TiO₂ (-4.0 eV).¹⁵ Hence, an effective electron injection from the excited dye to the TiO₂ is ensured. The HOMO levels were -5.19 and -5.25 eV, respectively, sufficiently lower than the iodide/triiodide redox couple (-4.83 eV vs vacuum). And it will be sufficient for the regeneration of the oxidized dye. Both the dyes exhibit two absorption peaks. The short-wavelength band appearing in 340 nm is assigned to the $\pi-\pi^*$ electron transition and the long-wavelength band appearing in the range of 450–500 nm is assigned to the charge-transfer transition between the triphenylamine dimer and cyanoacrylic segments, which produce the efficient charge-separation excited

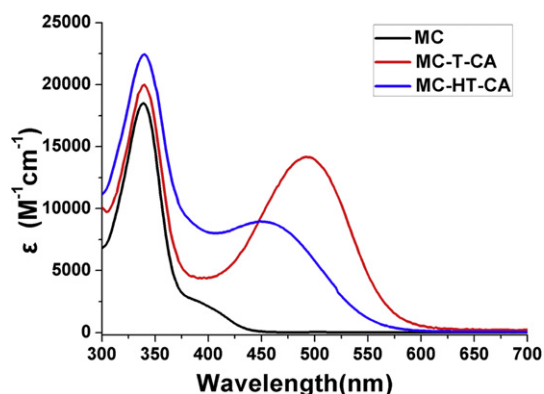


Fig. 2. Absorption spectra of MC and organic dyes in dichloromethane.

state.⁴ Compared to the dye, which contained a triphenylamine monomer, the absorption center of MC-T-CA is red shifted from 463 nm to 492 nm.¹⁶ However, the absorption maximum is blue-shifted by 42 nm when the hexyl chain is introduced. This result can be presumably ascribed to the reduced conjugation degree caused by the large steric hindrance effect of hexyl group. Previously, J. Nishida and his co-workers had observed the similar phenomena,¹⁷ and in their report, they ascribed the blue-shifted absorption band to the twisted molecular structure resulted from the introduction of large alkyl chain. The absorption spectra of the two dyes adsorbed onto the surface of TiO₂ were shown in Fig. 4. Compared to that in solutions, the absorption spectra of MC-T-CA and MC-HT-CA have blue-shifted by 23 and 38 nm. That may come from dye–TiO₂ interactions or deprotonation of the dyes at the surface of the TiO₂ film.⁴

To verify our result, molecular geometry optimization were carried out at the density functional theory (DFT) level using Gaussian 03 program package.¹⁸ And we found that dihedral angle

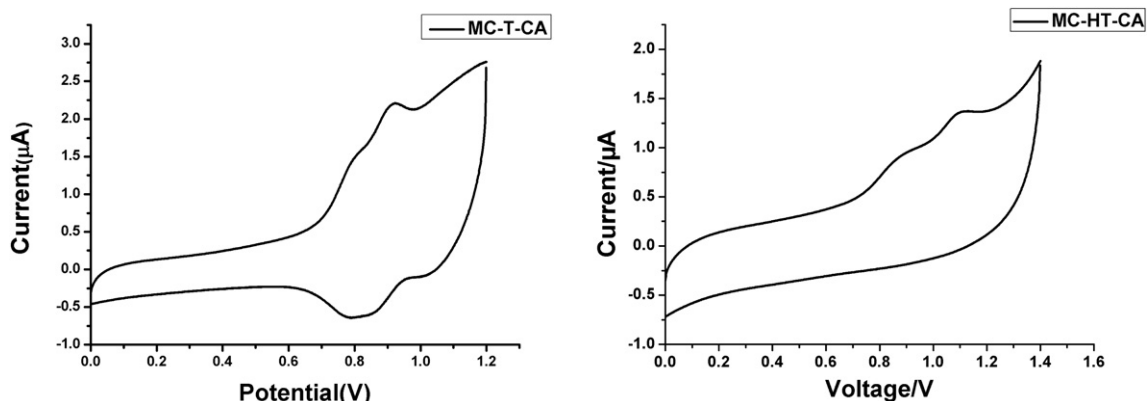


Fig. 3. Cyclic voltammogram measurements of MC-T-CA and MC-HT-CA.

Table 1
Optical and electrochemical properties of the new dyes

Entry	$\lambda_{\max}^a/\text{nm}(\epsilon/\text{M}^{-1}\text{cm}^{-1})$	$E_{\text{ox1}}^b/\text{V}$	HOMO ^c /eV	E_{0-0}^d/eV	LUMO ^e /eV
MC-T-CA	340(22,500)	0.79	−5.19	2.17	−3.02
	492(16,000)				
MC-HT-CA	340(20,000)	0.85	−5.25	2.25	−3.00
	450(8000)				

^a Absorption spectra were measured in Dichloromethane.

^b The potentials were got from cyclic voltammogram measurements (vs Ag/AgCl).

^c The HOMO levels were calibrated by the potentials vs Ag/AgCl.

^d E_{0-0} values were estimated from the edge of absorption spectra.

^e Calculated from the bandgap and HOMO value.

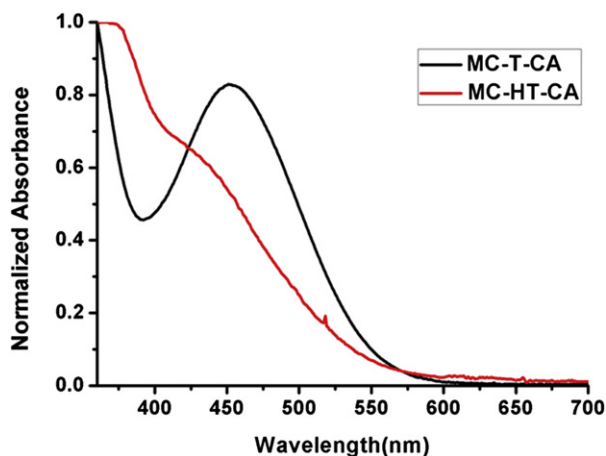


Fig. 4. Absorption spectra of the organic dyes adsorbed on TiO₂ surface.

between thiophene ring and the mean plane of the macrocycle became quite larger in the MC-HT-CA compared to that of MC-T-CA, the dihedral angle between thiophene and macrocycle is 49.11° for MC-T-CA, but it increases to 71.45° for MC-HT-CA, which meant a more twisted conformation. So a larger energy would be required to stimulate the intramolecular charge transfer. That is well account for the weak and blue-shifted maximum absorption band in MC-HT-CA. Moreover, as depicted in the optimized molecular conformation (Fig. 5), the HOMOs were localized on the triphenylamine macrocycle in both the two dyes, while the LUMOs were distributed over the cyanoacrylic acid and the adjacent benzene. This confirms the charge transfer type (HOMO–LUMO) reflected in the absorption spectra, which is consistent with the aforementioned experimental results.

The photovoltaic properties of the newly synthesized dyes are summarized in Table 2. All measurements were performed under

AM 1.5 irradiation (100 mW cm^{−2}) with 0.9 cm² active surface area defined by a metal mask. The incident photon-to-current efficient curves are shown in Fig. 6. It can be seen that the photocurrent response of MC-T-CA sensitized DSC is better due to the IPCE exceeding 70% in the range of 420–480 nm, and the maximum IPCE (85%) was obtained at 450 nm. When light absorption and reflection by the conducting glass are taken into account, this may correspond to almost the unity quantum yield. MC-HT-CA also shows a good photocurrent response with the maximum IPCE value of 76% at 425 nm. Both the IPCE spectra of the two dyes are consistent with their absorption spectra. The decrease of the IPCE above 600 nm toward the long-wavelength region is ascribed to the decrease of light harvesting for both dyes.

Measurement were performed under AM 1.5 irradiation on the DSC devices with 0.25 cm² active surface area defined by a metal mask. J_{sc} , short circuit current; V_{oc} , open circuit voltage; FF, fill factor; η , conversion efficiency.

Fig. 7 shows the I – V curves of DSSCs based on the as-synthesized dyes. Consistent with the result of IPCE and absorption spectra, MC-T-CA also shows better photovoltaic properties. Its overall conversion efficiency reaches 6.31%, which was obtained with $J_{\text{sc}}=12.47\text{ mA cm}^{-2}$, $V_{\text{oc}}=720\text{ mV}$, and $\text{ff}=0.69$. The V_{oc} and ff values derived from both newly synthesized dyes are even higher than those of device based on N3 measured at the same conditions. This benefits from the molecular structures of the two dyes, and the introduction of the macrocyclic triphenylamine is thought to be the main reason for the excellent performances. And it has been proved that high V_{oc} were closely related with retardation of charge recombination,¹⁹ either from injected electrons with the oxidized dye or with the oxidized electrolyte.¹⁷ More thorough research will be carried out in our next work. The macrocyclic triphenylamine acts not only as a secondary electron-donating group, which would retard the rate of charge recombination by increasing the distance between the dye cation center and the TiO₂ surface,¹² but it may be very favorable for the stabilization of the initially formed radical cation since it exhibits good intramolecular electron charge transfer.

As shown in Fig. 7, the dye MC-T-CA also shows higher short circuit current. The obviously higher photocurrent of MC-T-CA may be the result of its favorable absorption spectrum.²⁰ Thus, it can be inferred that a good absorption spectra is crucial for the photovoltaic performance since the V_{oc} and ff are almost equally high for the DSSCs based on our synthesized dyes. Interestingly, although the absorption spectra blue-shifted when a hexyl group is introduced to the thiophene unit, the V_{oc} of the DSSCs based on the dye keeps at a quite high level. Based on it, we could tune the absorption spectra by properly modifying the linker unit without lowering the V_{oc} value. The further research is still in progress.

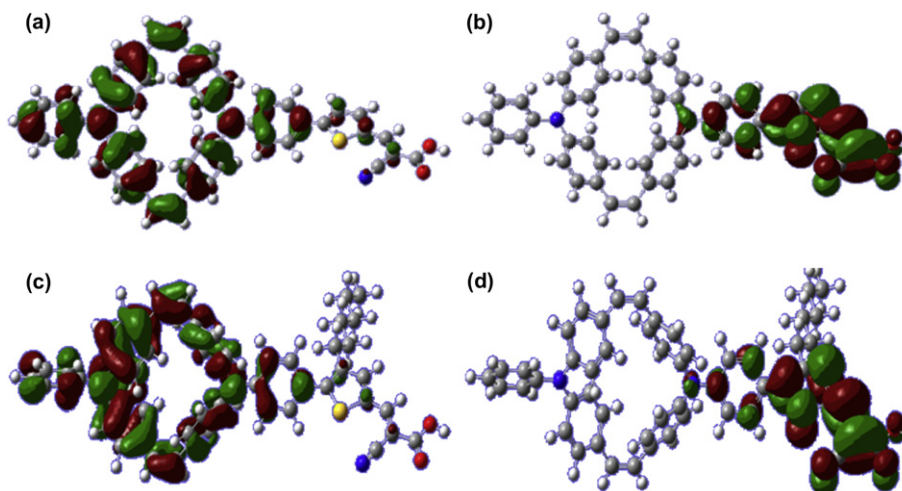


Fig. 5. The molecular conformation of the two dyes. HOMO (a), LUMO (b) of MC-T-CA, and HOMO (c), LUMO (d) of MC-HT-CA, respectively.

Table 2
Photovoltaic parameters of DSCs based on the new dyes

Dyes	$J_{sc}/\text{mA}/\text{cm}^2$	V_{oc}/mV	FF	$\eta/\%$
MC-T-CA	12.47	736	0.69	6.31
MC-HT-CA	9.81	720	0.68	4.79
N3	18.33	656	0.62	7.49

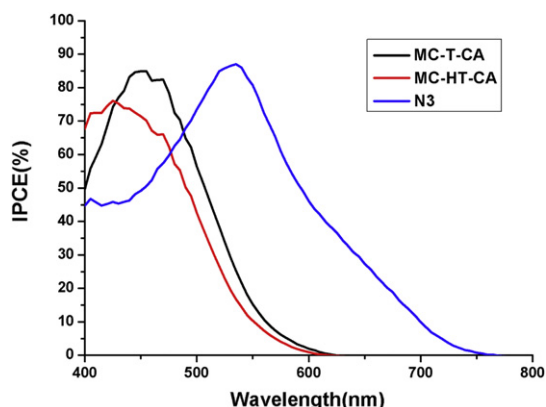


Fig. 6. IPCE spectra for the DSSCs based on MC-T-CA, MC-HT-CA and N3 [ruthenium(II) *cis*-(2,2'-bipyridyl-4,4'-dicarboxylate)₂(NCS)₂].

3. Conclusion

In summary, we have developed a novel type of highly efficient organic sensitizer using macrocyclic triphenylamine dimer as electron donor moiety, yielding maximum 85% IPCE and 6.31% power conversion efficiency. Introduction of a macrocyclic triphenylamine group as the electron-donor unit brought about improved photovoltaic performance, with V_{oc} and ff even better than those of N3. This result demonstrates that the macrocyclic triphenylamine dimer is a good candidate as donor unit for dye molecular design for DSSCs.

4. Experimental section

4.1. Compound synthesis

4.1.1. 2-Bromo-5-formylthiophene²¹ (**4**). To the cold solvent dry DMF (20 ml) at 0 °C, POCl₃ (18 ml) was added dropwise.

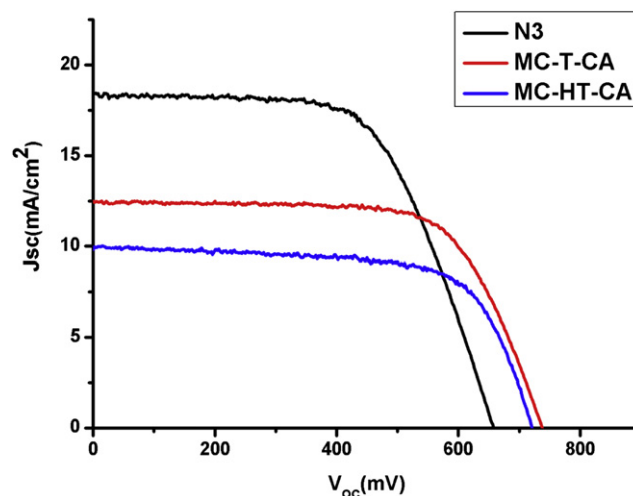


Fig. 7. Photocurrent density–photovoltage curves of MC-T-CA and MC-HT-CA.

The solution was stirred for 1 h. Then 2-bromothiophene (**3**) (1.94 ml, 20 mmol) dissolved in 1,2-dichloroethane (30 ml) was injected. The reaction was kept at 90 °C for 4 h under N₂. After cooling to room temperature, the reaction mixture was poured to 200 ml ice water, neutralized with saturated NaOH solution, and then extracted with dichloromethane twice. The combined organic layer was washed with H₂O and brine, dried over Na₂SO₄, and evaporated under reduced pressure. The crude product was purified by column chromatography (petroleum/EtOAc=5/1) to obtain compound **4** (3196 mg, 84.1%) as yellow liquid. MS(EI): m/z =190 (M⁺). ¹H NMR (CDCl₃, 400 MHz) δ /ppm: 9.78 (s, 1H), 7.52 (d, 1H), 7.19 (d, 1H).

4.1.2. 2-(4,4,5,5-Tetramethyl-1,3,2-dioxaborolan-2-yl)-thiophene-5-carbaldehyde²² (**5**). A solution of **4** (1.68 g, 8.8 mmol), bis(pinacolato)diboron (3.4 g, 13.2 mmol), PdCl₂(dppf) (756 mg, 0.88 mmol), and KOAc (2.587 g, 26.4 mmol) in degassed 1,4-dioxane (60 ml) was stirred at 80 °C for 6 h under N₂. The reaction was quenched by adding water, and extracted by dichloromethane. The organic phase was dried over Na₂SO₄, and concentrated under reduced pressure. The crude product was purified by silica gel chromatography (petroleum/dichloromethane=1/3) to give compound **5** (1.86 g, 88.9%) as yellow solid. Mp: 73 °C. MS(EI): m/z =238 (M⁺). ¹H

NMR (CDCl₃, 400 MHz) δ /ppm: 9.92 (s, 1H), 7.73 (d, H), 7.43 (d, 1H), 1.34 (s, 12H).

4.1.3. *N,N'*-Diphenyl-4-bromoaniline dimer⁸(**6**). It was prepared according to literature procedure with a little modification. Mp: >300 °C ¹H NMR (400 MHz, THF-*d*₄) δ 7.18 (d, 4H); 6.88 (d, 8H); 6.78–6.82 (m, 12H); 6.48 (s, 4H). ¹³C NMR (100 MHz, THF-*d*₄) δ (ppm) 147.96, 133.31, 132.15, 130.66, 130.38, 125.03, 123.29; HRMS(ESI): calcd for C₄₀H₂₈Br₂N₂ 696.0599, found: 696.0606 (M⁺).

4.1.4. *Compound (7)*.²³ A solution of compound **6** (350 mg, 0.5 mmol), compound **5** (760 mg, 3 mmol), Pd(OAc)₂ (20 mg, 0.1 mmol), Ligand (80 mg, 0.2 mmol), and CsF (220 mg, 1.5 mmol) in degassed 1,4-dioxane (50 ml) was stirred at 110 °C for 20 h under N₂. The reaction was quenched by adding water, and extracted by dichloromethane. The organic phase was dried over Na₂SO₄, and concentrated under reduced pressure. The crude product was purified by silica gel chromatography (petroleum/dichloromethane=1/1) to give compound **7** (76 mg, 23.5%) as orange solid. Mp>300 °C ¹H NMR (400 MHz, CDCl₃) δ 9.85 (s, 1H); 7.70 (d, 1H); 7.48 (d, 2H); 7.28 (d, 1H); 7.20 (t, 2H); 7.07–7.02 (m, 8H); 6.96 (d, 8H); 6.93–6.89 (m, 5H); 6.60 (s, 4H). ¹³C NMR (100 MHz, CDCl₃) δ /ppm: 182.70, 154.84, 148.23, 148.07, 147.22, 146.76, 141.35, 137.85, 133.70, 132.40, 131.96, 131.03, 130.99, 130.76, 130.62, 130.46, 130.10, 129.17, 127.38, 126.07, 125.77, 125.42, 124.97, 122.83, 121.84, 120.98. HRMS(ESI): calcd for C₄₅H₃₂N₂O₅ 648.2235, found: 648.2239 (M⁺).

4.1.5. *Compound (1)*.²¹ Compound **7** (70 mg, 0.1 mmol), cyanoacetic acid (50 mg, 0.5 mmol), and piperidine (100 μ l) were added to CHCl₃ (30 ml). The solution was stirred at 80 °C for 6 h. The reaction was quenched by adding water, and extracted by dichloromethane. The organic phase was dried over Na₂SO₄, and concentrated under reduced pressure. The crude product was purified by silica gel chromatography (first acetone/dichloromethane=1/1, then acetic acid) to give compound **1** (72 mg, 93.2%) as red solid. Mp>300 °C. ¹H NMR (400 MHz, CDCl₃) δ /ppm: 8.27 (s, 1H), 7.72 (d, 1H), 7.53 (d, 2H), 7.31 (d, 1H), 7.21 (t, 2H), 7.06–7.02 (m, 8H), 6.97 (d, 8H), 6.92–6.89 (m, 5H), 6.60 (s, 4H). ¹³C NMR (100 MHz, CDCl₃) δ /ppm: 148.21, 147.16, 146.73, 133.53, 132.40, 130.65, 130.62, 130.13, 129.17, 128.37, 127.28, 125.44, 125.36, 125.00, 121.80, 120.80. HRMS(ESI): calcd for C₄₈H₃₃N₃O₂S 715.2293, found: 715.2300 (M⁺).

4.1.6. *2-Bromo-3-hexyl-5-formylthiophene (9)*. To the cold solvent dry DMF (25 ml) at 0 °C, POCl₃ (22.5 ml) was added dropwise. The solution was stirred for 1 h. Then 2-bromothiophene (**8**) (3.31 g, 13.4 mmol) dissolved in 1,2-dichloroethane (30 ml) was injected. The reaction was kept at 90 °C for 4 h under N₂. After cooling to room temperature, the reaction mixture was poured to 200 ml ice water, neutralized with saturated NaOH solution, and then extracted with dichloromethane twice. The combined organic layer was washed with H₂O and brine, dried over Na₂SO₄, and evaporated under reduced pressure. The crude was purified by column chromatography (petroleum/EtOAc=5/1) to obtain compound **9** (3.217 g, 87.3%) as yellow liquid. MS(EI): *m/z*=274 (M⁺). ¹H NMR (400 MHz, CDCl₃) δ : 9.75 (s, 1H), 7.16 (s, 1H), 2.60 (t, 2H), 1.62–1.57 (m, 2H), 1.36 (m, 6H), 0.88 (t, 3H).

4.1.7. *2-(4,4,5,5-Tetramethyl-1,3,2-dioxaborolan-2-yl)-3-hexylthiophene-5-carbaldehyde*²² (**10**). A solution of **9** (2.72 g, 10 mmol), bis(pinacolato)diboron (5.08 g, 20 mmol), PdCl₂(dppf) (860 mg, 1 mmol), and KOAc (3.94 g, 30 mmol) in degassed 1,4-dioxane (80 ml) was stirred at 80 °C for 6 h under N₂. The reaction was quenched by adding water, and extracted by dichloromethane. The organic phase was dried over Na₂SO₄, and concentrated under reduced pressure. The crude product was purified by silica gel

chromatography (petroleum/dichloromethane=1/3) to give compound **10** (2.78 g, 86.3%) as yellow liquid. MS (EI): *m/z*=322. ¹H NMR (400 MHz, CDCl₃) δ : 9.90 (s, 1H), 7.63 (s, 1H), 2.87 (t, 2H), 1.59–1.56 (m, 2H), 1.34 (s, 12H), 1.31–1.29 (m, 6H), 0.87 (t, 3H).

4.1.8. *Compound (11)*.²³ A solution of compound **6** (350 mg, 0.5 mmol), compound **10** (970 mg, 3 mmol), Pd(OAc)₂ (20 mg, 0.1 mmol), Ligand (80 mg, 0.2 mmol), and CsF (220 mg, 1.5 mmol) in degassed 1,4-dioxane (50 ml) was stirred at 110 °C for 20 h under N₂. The reaction was quenched by adding water, and extracted by dichloromethane. The organic phase was dried over Na₂SO₄, and concentrated under reduced pressure. The crude product was purified by silica gel chromatography (petroleum/dichloromethane=1/1) to give compound **11** (79 mg, 21.5%) as orange solid. Mp>300 °C ¹H NMR (400 MHz, CDCl₃) δ 9.83 (s, 1H); 7.63 (d, 1H); 7.29 (d, 2H); 7.20 (t, 2H); 7.09–7.02 (m, 8H); 7.0–6.95 (m, 8H); 6.92–6.88 (m, 5H); 6.60 (s, 4H), 2.70 (t, 2H), 1.65–1.59 (m, 2H), 1.35–1.28 (m, 6H), 0.89 (t, 3H). ¹³C NMR (100 MHz, CDCl₃) δ 180.33, 146.91, 146.31, 146.14, 145.86, 145.37, 139.82, 138.08, 137.12, 132.12, 130.55, 129.07, 128.52, 128.35, 127.54, 124.97, 123.81, 123.34, 121.69, 120.32, 119.30, 30.30, 29.30, 27.72, 27.22, 21.19, 12.14. HRMS(ESI): calcd for C₅₁H₄₄N₂O₅ 732.3174, found 732.3178.

4.1.9. *Compound (2)*.²¹ Compound **11** (70 mg, 0.1 mmol), cyanoacetic acid (50 mg, 0.5 mmol), and piperidine (100 μ l) were added to CHCl₃ (30 ml). The solution was stirred at 80 °C for 6 h. The reaction was quenched by adding water, and extracted by dichloromethane. The organic phase was dried over Na₂SO₄, and concentrated under reduced pressure. The crude product was purified by silica gel chromatography (first acetone/dichloromethane=1/1, then acetic acid) to give compound **1** (72 mg, 93.2%) as red solid. Mp>300 °C. ¹H NMR (400 MHz, CDCl₃) δ ppm: 8.27 (s, 1H), 7.71 (s, 1H), 7.65 (d, 2H), 7.21 (t, 2H), 7.07–7.02 (m, 8H), 7.00–6.96 (m, 8H), 6.91–6.87 (m, 5H), 6.59 (s, 4H), 2.38 (t, 2H), 1.66–1.60 (m, 2H), 1.30–1.26 (m, 6H), 0.90 (t, 3H). ¹³C NMR (100 MHz, CDCl₃) δ ppm: 148.39, 147.48, 146.90, 132.59, 130.78, 130.65, 130.34, 130.25, 130.14, 130.12, 130.06, 129.35, 125.52, 125.16, 121.99, 120.82, 32.26, 31.57, 29.69, 29.66, 23.02, 14.44. HRMS(ESI): calcd for C₅₄H₄₅N₃O₂S 799.3232, found: 799.3236 (M⁺).

4.2. Computational methodology

To get further insight into the molecular structure and electron distribution of **MC-T-CA** and **MC-HT-CA**, molecular calculations were carried out with the Gaussian 03 program package. Equilibrium ground state geometry and electronic properties of basic unit of the dyes were optimized by means of the density functional theory (DFT) method at the B3LYP level of theory (Becke-style three-parameter density functional theory using the Lee–Yang–Par correlation functional) with the 6-31G(d,p) basic set.

4.3. Electrochemical properties

Cyclic voltammetric measurements were recorded on a CHI660C voltammetric analyzer (CH Instruments, USA). They were carried out in a conventional three-electrode cell using Pt button working electrodes in 0.1 M dry dichloromethane solution of (*n*-Bu)₄NPF₆, a platinum wire counter electrode, and an Ag/AgCl reference electrode at room temperature.

4.4. DSSC device fabrication

For fabrication of the devices,²⁴ two layers of TiO₂, the main layer, and the scattering layer, were prepared by screen-printing TiO₂ pastes on FTO glass substrate (10 Ω /sq, Nippon Sheet Glass). The main layer (thickness, 14 μ m; TiO₂ particle size, 18 nm) and scattering layer (thickness, 8 μ m; TiO₂ particle size, 400 nm) were

prepared from two different TiO₂ colloids (PST-18NR and PST-400C from CCI in Japan). After screen-printing, the TiO₂ film was heated at 500 °C for 30 min and treated with 0.04 M TiCl₄ aqueous solution. The two new dyes and **N3** dye solutions were prepared in DMF at a concentration of 0.5 mM. A solution of 1 mM chenodeoxycholic acid in *tert*-butyl alcohol/acetonitrile (1:1, v/v) was prepared, the use of which is able to effectively prevent unfavorable dye aggregation on TiO₂ surface. The TiO₂ films were left in the solution at room temperature for 15 h. A Pt-sputtered FTO glass was used as a counter electrode. The electrolyte was composed of 0.6 M 1-propyl-3-methylimidazolium iodide, 0.1 M LiI, 0.05 M I₂, and 0.75 M *tert*-butylpyridine in a mixture of acetonitrile and valeronitrile (1:1, v/v). The photovoltaic performance of the devices was recorded under 100 mW/cm² simulated air mass (AM) 1.5 solar light illumination.

Acknowledgements

The authors are grateful to financial support from the National Natural Science Foundation of China (20952001, 21021091), the State Key Basic Research Program (2011CB808401), and the Chinese Academy of Sciences.

References and notes

- Oregan, B.; Gratzel, M. *Nature* **1991**, *353*, 737–740.
- Gao, F.; Wang, Y.; Shi, D.; Zhang, J.; Wang, M. K.; Jing, X. Y.; Humphry-Baker, R.; Wang, P.; Zakeeruddin, S. M.; Gratzel, M. *J. Am. Chem. Soc.* **2008**, *130*, 10720–10728.
- Koumura, N.; Wang, Z. S.; Mori, S.; Miyashita, M.; Suzuki, E.; Hara, K. *J. Am. Chem. Soc.* **2006**, *128*, 14256–14257.
- Thomas, K. R. J.; Baheti, A.; Singh, P.; Lee, C. P.; Ho, K. C. *J. Org. Chem.* **2011**, *76*, 4910–4920.
- Lee, J. K.; Yang, M. J. *Mater. Sci. Eng., B* **2011**, *176*, 1142–1160.
- Qu, S. Y.; Hua, J. L.; Tian, H. *Sci. China: Chem.* **2012**, *55*, 677–697.
- Ning, Z. J.; Zhang, Q.; Wu, W. J.; Pei, H. C.; Liu, B.; Tian, H. *J. Org. Chem.* **2008**, *73*, 3791–3797.
- Song, Y. B.; Di, C. A.; Yang, X. D.; Li, S. P.; Xu, W.; Liu, Y. Q.; Yang, L. M.; Shuai, Z. G.; Zhang, D. Q.; Zhu, D. B. *J. Am. Chem. Soc.* **2006**, *128*, 15940–15941.
- Memminger, K.; Oeser, T.; Muller, T. J. *J. Org. Lett.* **2008**, *10*, 2797–2800.
- Ning, Z. J.; Tian, H. *Chem. Commun.* **2009**, 5483–5495.
- Ito, S.; Liska, P.; Comte, P.; Charvet, R. L.; Pechy, P.; Bach, U.; Schmidt-Mende, L.; Zakeeruddin, S. M.; Kay, A.; Nazeeruddin, M. K.; Gratzel, M. *Chem. Commun.* **2005**, 4351–4353.
- Clifford, J. N.; Martinez-Ferrero, E.; Viterisi, A.; Palomares, E. *Chem. Soc. Rev.* **2011**, *40*, 1635–1646.
- Numata, Y.; Ashraful, I.; Shirai, Y.; Han, L. Y. *Chem. Commun.* **2011**, *47*, 6159–6161.
- Zhao, Y.; Ye, C. Q.; Qiao, Y. L.; Xu, W.; Song, Y. L.; Zhu, D. B. *Tetrahedron* **2012**, *68*, 1547–1551.
- Tang, C. W. *Appl. Phys. Lett.* **1986**, *48*, 183–185.
- Shen, P.; Liu, Y. J.; Huang, X. W.; Zhao, B.; Xiang, N.; Fei, J. J.; Liu, L. M.; Wang, X. Y.; Huang, H.; Tan, S. T. *Dyes Pigm.* **2009**, *83*, 187–197.
- Nishida, J.; Masuko, T.; Cui, Y.; Hara, K.; Shibuya, H.; Ihara, M.; Hosoyama, T.; Goto, R.; Mori, S.; Yamashita, Y. *J. Phys. Chem. C* **2010**, *114*, 17920–17925.
- Frisch, M. J.; Trucks, G. W.; Schlegel, H. B.; Scuseria, G. E.; Robb, M. A.; Cheeseman, J. R.; Montgomery, J. A., Jr.; Vreven, T.; Kudin, K. N.; Burant, J. C.; Millam, J. M.; Iyengar, S. S.; Tomasi, J.; Barone, V.; Mennucci, B.; Cossi, M.; Scalmani, G.; Rega, N.; Petersson, G. A.; Nakatsuji, H.; Hada, M.; Ehara, M.; Toyota, K.; Fukuda, R.; Hasegawa, J.; Ishida, M.; Nakajima, T.; Honda, Y.; Kitao, O.; Nakai, H.; Klene, M.; Li, X.; Knox, J. E.; Hratchian, H. P.; Cross, J. B.; Bakken, V.; Adamo, C.; Jaramillo, J.; Gomperts, R.; Stratmann, R. E.; Yazyev, O.; Austin, A. J.; Cammi, R.; Pomelli, C.; Ochterski, J. W.; Ayala, P. Y.; Morokuma, K.; Voth, G. A.; Salvador, P.; Dannenberg, J. J.; Zakrzewski, V. G.; Dapprich, S.; Daniels, A. D.; Strain, M. C.; Farkas, O.; Malick, D. K.; Rabuck, A. D.; Raghavachari, K.; Foresman, J. B.; Ortiz, J. V.; Cui, Q.; Baboul, A. G.; Clifford, S.; Cioslowski, J.; Stefanov, B. B.; Liu, G.; Liashenko, A.; Piskorz, P.; Komaromi, I.; Martin, R. L.; Fox, D. J.; Keith, T.; Al-Laham, M. A.; Peng, C. Y.; Nanayakkara, A.; Challacombe, M.; Gill, P. M. W.; Johnson, B.; Chen, W.; Wong, M. W.; Gonzalez, C.; Pople, J. A. *Gaussian 03, Revision B.04*; Gaussian: Wallingford, CT, 2004.
- Ning, Z. J.; Zhang, Q.; Pei, H. C.; Luan, J. F.; Lu, C. G.; Cui, Y. P.; Tian, H. *J. Phys. Chem. C* **2009**, *113*, 10307–10313.
- Hagberg, D. P.; Marinado, T.; Karlsson, K. M.; Nonomura, K.; Qin, P.; Boschloo, G.; Brinck, T.; Hagfeldt, A.; Sun, L. *J. Org. Chem.* **2007**, *72*, 9550–9556.
- Wang, P.; Wang, M. K.; Xu, M. F.; Shi, D.; Li, R. Z.; Gao, F. F.; Zhang, G. L.; Yi, Z. H.; Humphry-Baker, R.; Zakeeruddin, S. M.; Gratzel, M. *Adv. Mater.* **2008**, *20*, 4460–4463.
- Sonar, P.; Singh, S. P.; Leclere, P.; Surin, M.; Lazzaroni, R.; Lin, T. T.; Dodabalapur, A.; Sellinger, A. *J. Mater. Chem.* **2009**, *19*, 3228–3237.
- Pratap, R.; Parrish, D.; Gunda, P.; Venkataraman, D.; Lakshman, M. K. *J. Am. Chem. Soc.* **2009**, *131*, 12240–12249.
- Jiang, K. J.; Li, G.; Li, Y. F.; Li, S. L.; Yang, L. M. *J. Phys. Chem. C* **2008**, *112*, 11591–11599.